CF- 2984
April 24, 1962
COPY NO. 44

FLUTTER SIMULATION

by

J. P. Kearns

THE JOHNS HOPKINS UNIVERSITY
APPLIED PHYSICS LABORATORY
8621 GEORGIA AVENUE SILVER SPRING, MARYLAND

Operating under Contract NOrd 7386 with the Bureau of Naval Weapons, Department of the Navy

The Johns Hopkins University
APPLIED PHYSICS LABORATORY
Silver Spring, Maryland

CF-2984

Flutter Simulation

by

J. P. Kearns

The Johns Hopkins University
APPLIED PHYSICS LABORATORY
Silver Spring, Maryland

TABLE OF CONTENTS

LIST OF SYMBOLS

c	Plate chord
b	Plate semi-chord
l	Plate span
t	Plate thickness
EI	Plate bending rigidity $\cong \frac{Ect^3}{12}$
GJ	Plate torsional rigidity $\cong \frac{1}{3}\ Gct^3$
x	Chordwise coordinate
y	Spanwise coordinate
D_h	Spanwise bending mode shape
D_α	Torsional mode shape
m	Spanwise mass distribution, lb $sec^2/in.^2$
i_p	Spanwise polar moment of inertia distribution, lb sec^2
$\bar{x}$	Distance from c.g. of an element to the elastic axis of a surface
$\bar{r}$	Radius of gyration of a given segment
ρ	Air density
μ	$m/4\rho b^2$ mass ratio parameter
$k_h g_h$	Structural damping in bending
$c_h \omega$	Aerodynamic damping parameter in bending
$k_\alpha g_\alpha$	Structural damping in torsion
$c_\alpha \omega$	Aerodynamic damping parameter in torsion
q_h	Generalized coordinate in bending
q_α	Generalized coordinate in torsion
P_a	Shaker force
$C_{L\alpha}$	Lift coefficient ($L = C_{L\alpha} q_d A\alpha$) Flat Plate $C_{L\alpha} = \frac{4}{\sqrt{M^2-1}}$
$N q_\alpha$	Generalized aerodynamic force ($N q_\alpha = \left[\int_0^l (C_{L\alpha}\ q_d\ D_h\ D_\alpha\ c\ dy)\right] q_\alpha$
q_d	Dynamic pressure ($q_d = .7\ p\ M_m^2$)

M_m Mach number

k_h Generalized bending stiffness

$$\int_0^{\ell} EI \left(\frac{d^2 D_h}{dy^2} \right)^2 dy$$ for cantilever beam, three-dimensional system

or k_h, basic translational spring stiffness, two-dimensional system.

k_α Generalized torsional stiffness

$$\int_0^{\ell} GJ \left(\frac{d\, D_\alpha}{dy} \right)^2 dy$$ for cantilever beam, three-dimensional system

or k_α , basic pitching spring stiffness, two-dimensional system.

I_h Generalized inertia in bending

$$\int_0^{\ell} m\, D_h^2\, dy$$ for cantilever beam

or M_c, concentrated mass, two-dimensional system.

I_α Generalized inertia in twisting

$$\int_0^{\ell} i_p\, D_\alpha^2\, dy,$$ for cantilever torsion

I_α, concentrated polar moment of inertia two-dimensional system.

S Generalized mass unbalance

$$\int_0^{\ell} m\, \bar{x}\, D_h\, D_\alpha\, dy,$$ for a distributed mass system

$M\bar{x}$ for a two-dimensional system.

h Linear displacement of mid-chord, positive downward ($h = D_h\, q_h$)

α Angular displacement, positive stalling ($\alpha = D_\alpha\, q_\alpha$)

ω_h Uncoupled bending frequency

ω_α Uncoupled torsional frequency

i Current through the electromechanical shaker

λ Ratio of shaker force to current

l_p Perpendicular distance from mirror to photocell

δ Image motion relative to the photocell

OBJECTIVES

1. Flutter simulation is a closed loop ground vibration to find flutter speeds on actual missile wings. The elements in a closed loop convert the wing linear and angular motions into electro-mechanical forces which simulate the aerodynamic forces generated by the motions in supersonic flight at some chosen Mach number and altitude. If the closed loop becomes unstable, it is inferred that the missile surface would become unstable in flight.

RESULTS

The results are developed in terms of what can be accomplished using one shaker delivering a concentrated force in response to one particular pitching angle on a wing. This is a necessary first step toward a system of shakers to represent the distributed airforces which are functions of the linear and angular displacements and velocities.

Studies of a missile wing flutter problem by Dr. E. Shotland and Dr. A. Mitchell were made in 1952 with the drastic simplification of the airforces which is embodied in the one-channel simulator system. A check on some two-dimensional translation-pitch flutter cases for which classical NACA results were available led to the tentative conclusion that the lift force per unit angle was the most significant coefficient in the flutter problem.

To get a one-channel system, four major components were needed: (1) An angular displacement transducer, (2) a preamplifier to raise the signal level; (3) a power amplifier and (4) an electro-mechanical shaker. Various designs for these components were used in the flutter simulation of two aluminum cantilever plates, a 30" x 12" x .125" plate A, and a 15.5" x 10" x .25" plate B.

It should be noted that component (1), the angular transducer, posed a durable problem. It was difficult on plate A to match the gains of two pick-ups, the differential output being the pitch angle signal. A number of angular transducers were tested t obtain quantitative simulation for the second plate. The best device was an electro-optical angular pickup and an associated pre-amplifier. For the one-channel system as a whole a shaker force per unit pitch angle up to 17000 lb/radian over a frequency band from 0 to 500 cps is now available. It has been used to produce flutter simulation of the second plate, and predicts a flutter Mach No. of 2.9 at sea level. A number of qualifications are needed on this prediction, none of which bear on the validity of the one-channel feedback loop as such. These qualifications arise from such issues as the choice of suitable airforce coefficients and the number of channels which are needed to simulate the coefficients.

The work serves to illustrate the performance of the one-channel system. It is recommended that evaluation of the system be continued. If it continues to behave well, it is recommended that another channel be added for further tests; a number of channels should be able to simulate both flutter and divergence. Finally, it is noted that the electro-optical angular pickup should find useful applications in the measurement of static and dynamic angular motions of structures in general.

DISCUSSION

The topics which follow cover the choice of airforce coefficients for simulation, and the details for the two-dimensional flutter analysis using the lift due to angle. The modification due to aerodynamic damping is shown. Vibration testing for special angle/force data is described for use in a direct calculation of flutter speed.

The theory is extended to cover the three-dimensional case of a cantilever plate. The concept for the finding direct flutter data from open-loop vibration testing is extended to the three-dimensional case. Closing this loop then simulates the flutter. The development problems for an early study of a Plate A and a recent study of a Plate B conclude the report.

1. Choice of Airforce Coefficients for Simulation

The objective is to make a limited number of ground test forces simulate the most important aerodynamic forces. The force which appears to be the most important is the lift due to angle of attack. This opinion is reached by doing simplified studies, of the sort reported in Section 2. The results are encouraging. The studies were originally made to check the assumption made by Dr. E. Shotland and Dr. A. K. Mitchell of the Applied Physics Laboratory for wing flutter analysis in 1951. Such assumptions allowed other complex factors to be introduced into the analyses, and exposed the effects of frequency ratio and mass balance. Piston theory was a later notable simplification by Ashby and Zartarian, made for the same reasons. In recent years, other flutter studies using simplified airforces have been reported, and much research is in progress on the subject.

Tests at APL using the one force due to angle of attack have been made on two cantilever plates, A and B. These tests prompted a review of the important airforces, and it is now believed that damping forces in the bending and twisting degrees of freedom are important. The ratio of the two generalized damping forces influences the flutter frequency, and hence the flutter speed. On plate B, (Figures 3 and 4) the damping force and moment are provided by two concentrated forces, one 3 inches ahead and the other 3 inches behind the elastic axis or mid-chord, 1/2 inch in from the tip. The dampers are not powerful enough to simulate the calculated generalized damping factors called for by piston theory,

but they do provide a step in the right direction. The lift coefficient C_L from piston theory is $\frac{4}{M}$, while the classical value is $\frac{4}{\sqrt{M^2-1}}$. It will be seen from the discussion, and particularly equation (32), that either value of C_{L_α} may be used to evaluate its effect on the altitude-Mach number flutter boundary.

2. Flutter Analysis - Two-Dimensional System

(a) One No-Lag Lift Force, No Damping

It is well be begin with a simple two-dimensional surface having bending and rotational degrees of freedom, reacting only to an aerodynamic force N_α at the elastic axis, Figure 1.

The equilibrium equations for sinusoidal oscillation are:

$$(k_{hT} - I_h \omega^2)\,\bar{h} - S\,\omega^2\,\bar{\alpha} = -N_\alpha \bar{\alpha} \tag{1}$$

$$-S\omega^2\,\bar{h} + (k_{\alpha T} - I_\alpha \omega^2)\,\bar{\alpha} = 0 \tag{2}$$

$$h = \bar{h} e^{i\omega t}$$
$$\alpha = \bar{\alpha} e^{i\omega t}$$
$$k_{hT} = k_h + i\,G_h$$
$$k_{\alpha T} = k_\alpha + i\,G_\alpha$$

A condition of flutter exists when the determinant is equal to zero.

$$k_{h_o} k_{\alpha_o} - G_h G_\alpha - \omega^2 \left[I_h k_{\alpha_o} + I_\alpha k_{h_o}\right] + I_h I_\alpha \omega^4 + S\,\omega^2 N_\alpha - S^2 \omega^4 + i\,G_\alpha \left[k_{h_o} - I_h \omega^2\right] + i\,G_h \left[k_\alpha - I_\alpha \omega^2\right] = 0 \tag{3}$$

The real and imaginary parts are separately set equal to zero:

$$k_\alpha\, g_\alpha \left[k_h - I_h \omega^2\right] = -\left[k_\alpha - I_\alpha \omega^2\right] K_h\, g_h \tag{4}$$

Assume:

$$g_h = g_\alpha$$

(5) $$\omega^2 = \frac{2\, k_\alpha\ k_h}{I_h\, k_\alpha + I_\alpha\, k_h}$$

Define:

$$\omega_\alpha^2 = \frac{k_\alpha}{I_\alpha} \qquad G_h = k_h\ g_h$$

$$\omega_h^2 = \frac{k_h}{I_h} \qquad G_\alpha = k_\alpha\ g_\alpha$$

(6) $$\omega^2 = \frac{2\, \omega_\alpha^2\, \omega_h^2}{\omega_\alpha^2 + \omega_h^2}$$

This value of the frequency is then used in the real part of the equation:

(7) $$k_h\ k_\alpha\left[1 - g_h\ g_\alpha\right] - \frac{2\, \omega_\alpha^2 \omega_h^2}{\omega_h^2+\omega_\alpha^2}\left[I_h\, k_\alpha + I_\alpha\, k_h\right] + I_h\, I_\alpha \frac{(4)\ \omega_\alpha^4\ \omega_h^4}{(\omega_\alpha^2+\omega_h^2)^2}$$

$$+ 2\, N\, S \frac{\omega_h^2\ \omega_\alpha^2}{\omega_h^2+\omega_\alpha^2} - 4\, S^2 \frac{\omega_h^4\ \omega_\alpha^4}{(\omega_h^2 + \omega_\alpha^2)^2} = 0$$

The equation ultimately simplifies to:

(8) $$\frac{N\, S}{I_h\ I_\alpha\ \omega_\alpha^2} = g^2\ \frac{\left[1 + \left[\frac{\omega_h}{\omega_\alpha}\right]^2\right]^2}{2} + \frac{\left[1 - \left(\frac{\omega_h}{\omega_\alpha}\right)^2\right]^2 + 4\, \frac{S^2}{I_h\ I_\alpha}\left(\frac{\omega_h}{\omega_\alpha}\right)^2}{2\left[1 + \left(\frac{\omega_h}{\omega_\alpha}\right)^2\right]}$$

The equation can be put into a form suitable for correlating results with NACA calculations in Reference (1) by using the definitions on page 2 and the ultimate result is:

$$(9) \qquad \frac{V_s}{b\,\omega_c} = \sqrt{\frac{\mu \frac{r^2}{x^2}\sqrt{M^2-1}}{\frac{x}{r}\,b} \cdot \frac{\left[1-\left(\frac{\omega_h}{\omega_c}\right)^2\right]^2 + 4\left(\frac{x}{r}\right)^2\left(\frac{\omega_h}{\omega_c}\right)^2}{2\left[1+\left(\frac{\omega_h}{\omega_c}\right)^2\right]}}$$

Table I, page 27 shows reasonable agreement of the results from this simplified theory with the "exact" NACA calculations.

(b) <u>One lift force plus damping in both degrees of freedom</u>

The comparison shown is for a theory in which the damping is entirely structural of the form i k g. Aerodynamic damping is viscous in nature; and an examination of the flutter determinant shows:

$$(10) \qquad \begin{vmatrix} k_h + i\left[G_h + C_h\,\omega\right] - I_h\,\omega^2 & N - S\,\omega^2 \\ -S\,\omega^2 & k_\alpha + i\left[G_\alpha + C_\alpha\,\omega\right] - I_\alpha\,\omega^2 \end{vmatrix} = 0$$

The flutter frequency is determined from the condition that the imaginary part of the expanded determinant is equal to zero.

$$(11) \qquad i\,C_{hT}\left[k_\alpha - I_\alpha\,\omega^2\right] + i\,C_{\alpha T}\left[k_h - I_h\,\omega^2\right] = 0$$

$$(12) \qquad \omega_f = \sqrt{\frac{k_h + \frac{C_{hT}}{C_{\alpha T}}\,k_\alpha}{I_h + \frac{C_{hT}}{C_{\alpha T}}\,I_\alpha}}$$

$$C_{hT} = G_h + C_h\,\omega_f$$

$$C_{\alpha T} = G_\alpha + C_\alpha\,\omega_f$$

The real part of the determinant should also vanish:

$$(13) \qquad (k_h - I_h \omega_f^2)(k_\alpha - I \omega_f^2) - C_{hT} C_{\alpha T} + S \omega_f^2 N - S^2 \omega_f^4 = 0$$

Thus it is possible to find the critical value of the aerodynamic coefficient needed to satisfy (13).

$$(14) \qquad N = \frac{-(k_h - I_h \omega_f^2)(k_\alpha - I_\alpha \omega_f^2) + C_{hT} C_{\alpha T}}{S \omega_f^2} + S \omega_f^2$$

The use of aerodynamic viscous damping results in the aerodynamic force coefficient N required for flutter, to be compared to Equation (8), where only structural damping of the form $i k g$ was present. In any given problem, two values of N may be computed, and the effect of the aerodynamic damping terms evaluated. The major effect arises from the ratio of the two damping factors, to judge from the example of Plate B.

The aerodynamic coefficients used in the analysis, namely N, $C_h \omega$ and $C_\alpha \omega$ are sufficient to describe the forces given by second order piston theory - Reference (2). Then the values are:

$$N = 4 \frac{\rho b V^2}{M_m} \ell$$

$$C_h \omega = + 4 \rho a b \omega \ell$$

$$C_\alpha \omega = + \frac{4}{3} \rho a b^3 \omega \ell$$

for forces at the mid-chord of a thin plate.

3. Ground Vibration Testing - Two Dimensional System

In special cases it has been shown that the simplified airforce theory with one lift force yields reasonable answers. Adding damping then in effect makes it a piston theory type analysis which has been thoroughly evaluated

in Reference (2). The question then arises: how can ground vibration testing on a "two-dimensional" wing lead to an estimate of flutter speed?

First place two concentrated damping forces on the wing which produce the coefficients C_h and C_α given by piston theory. Then apply a shaker force at the plate mid-chord. What relationship does that force have to an aerodynamic force N_α? What data are needed to compute flutter speed?

The two forces may be related by thinking of the following experiment. The sinusoidal ground test force produces a sinusoidal pitching angle (Fig. 2). It varies both in magnitude and phase relative to the driving force as the frequency is changed. At some special frequency (Test #1, Fig. 2), the pitching angle α_c may be 180 degrees out of phase with a downward shaking force. Next, allow very low density air to flow over the airfoil at a chosen supersonic Mach number (Test #2). At the instant when the shaker force is downward, the airfoil is pitching nose down; and the small airforce which is generated is downward, exactly in phase with the shaker force at the same point where the shaker force is applied. Under these circumstances, the sum of the shaker and aerodynamic forces increases the angular oscillation. Reduce the test shaker force such that the sum of the shaker and aerodynamic forces and the resultant angle of oscillation remain the same as before. For Test #3 allow the density of the airflow to be increased to a critical level, where it is observed that the shaker force is no longer needed to maintain the oscillation. A condition of flutter has been reached.

The magnitude of the aerodynamic force is thus equal to the shaker force which it fully replaces in causing the oscillation. It follows that the present aerodynamic force per unit angle of airfoil pitching is simply the shaker force per unit angle. It is now seen that this information is what is needed to make a flutter speed or Mach number estimate. The flutter Mach number at the chosen altitude will produce an aerodynamic force per unit angle equal to the shaker force per unit angle derived from direct ground vibration testing at zero airspeed.

It is desirable to underline the significance in the experiment of the requirement that the chosen frequency should be one in which the angle is 180 degrees out of phase with the test shaker force. If any other frequency

had been chosen, the phase of the angle, and the phase of the aerodynamic force due to the airflow, would not allow for the direct replacement of the portion of the test shaker force by the aerodynamic force.

The two-dimensional flutter Mach number is, according to the foregoing argument, one which satisfies the following equation.

$$\frac{P_s}{\alpha} = C_{L\alpha}\, q_d\, A \tag{15}$$

where:

$C_{L\alpha}$ = lift curve slope

q_d = dynamic pressure

A = area of airfoil

$C_{L\alpha} = \frac{4}{\sqrt{M_\infty^2 - 1}}$, conventional supersonic flat plate.

or

$C_{L\alpha} = \frac{4}{M_\infty}$, piston theory

4. Flutter Analysis - Three-dimensional System

Both the theoretical and the experimental discussions have been based on a two-dimensional system. It is useful to extend these concepts to a three-dimensional system, such as a clamped cantilever plate.

When the motion of the plate is idealized in terms of two degrees of freedom, primary bending, and primary torsion, the extension of the concept can proceed conveniently. Lagrange's equations are needed to define the plate motion. In general:

$$\frac{d}{dt}\left(\frac{\partial T}{\partial q_i}\right) + \frac{\partial V}{\partial q_i} = Q_i \tag{16}$$

where T is the kinetic energy of the system, V is the potential energy, and Q_i is the generalized force in the ith degree of freedom.

The displacement of the flexural axis of the plate, namely the midchord, is approximated by one degree of freedom.

$$h = D_h\, q_h \tag{17}$$

where D_h is the spanwise bending mode shape and q_h is the unknown time-varying function.

The angular displacement of the plate is approximated by another degree of freedom.

(18) $$\alpha = D_\alpha \; q_\alpha \text{ , where}$$

D_α is the primary torsional mode shape, and q_α is the unknown time-varying function in this degree of freedom.

The kinetic energy of the system is:

(19) $$T = \tfrac{1}{2} \int_0^\ell m \left(D_h \dot{q}_h + \bar{x}_p \, D_\alpha \dot{q}_\alpha\right)^2 dy + \frac{1}{2} \int_0^\ell i_p \, D_\alpha^2 \, \dot{q}_\alpha^2 \; dy$$
$$+ \tfrac{1}{2} \; M_b \left[D_{hb} \, \dot{q}_h + \bar{x}_b \, D_{\alpha b} \, \dot{q}_\alpha\right]^2$$

The potential energy of the system is:

(20) $$V = \tfrac{1}{2} \int_0^\ell EI \left(\frac{d^2 D_h}{dy^2}\right)^2 q_h^2 \, dy + \tfrac{1}{2} \int_0^\ell GJ \left(\frac{d \, D_\alpha}{dy}\right)^2 q_\alpha^2 \; dy$$

The variational work performed by an applied shaker force P_a at the mid-chord and by the forward and aft dampers is:

(21) $$\delta w = P_a \, \delta h_a + P_e \, \delta h_e + F_f \, \delta h_f$$

$$h_a = D_{ha} \, q_h$$
$$h_e = D_{he} \, q_h + x_e \, D_{\alpha e} \, q_\alpha$$
$$h_f = D_{hf} \, q_h + x_f \, D_{\alpha f} \, q_\alpha$$
$$P_a = A \, e^{i\omega t}$$
$$P_e = - \bar{C}_{he} \, \dot{h}_e$$
$$P_f = - \bar{C}_{hf} \, \dot{h}_f$$

When the shaker force is absent, and the surface is flying at some supersonic Mach number, the variational work performed by the simplified aerodynamic forces is:

$$(22) \qquad \delta w = \int_0^{\ell} \frac{\partial F}{\partial y} \quad (\delta h) \quad dy + \int_0^{\ell} \frac{\partial M}{\partial y} \quad (\delta \alpha) \quad dy$$

$$\frac{\partial F}{\partial y} = -C_{L\alpha} \, q_d \, c \, \alpha - \bar{c}_h \, \dot{h}$$

$$\frac{\partial M}{\partial y} = -\bar{c}_\alpha \, \dot{\alpha}$$

The application of Lagrange's Equations yields in the case of forced sinusoidal vibration:

$$(23) \qquad (k_h - I_h \omega^2 + i \, G_h) \, q_h - S \, \omega^2 \, q_\alpha = P_a \, D_{ha} - i \, C_h \, \dot{q}_h$$

$$- S \, \omega^2 \, q_h + (k_\alpha - I \, \omega^2 + i \, G_\alpha) \, q_\alpha = - i \, C_\alpha \, q_\alpha$$

With:

$$k_h = \int_0^{\ell} EI \left(\frac{d^2 \, D_h}{dy^2} \right)^2 dy, \quad \text{or } I_h \, \omega_{oh}^2$$

$$S = M_d \, \bar{x}_d \, D_{hd} \, D_{\alpha d}$$

$$k_\alpha = \int_0^{\ell} GJ \left(\frac{d \, D_\alpha}{dy} \right)^2 dy, \quad \text{or } I_\alpha \, \omega_{o\alpha}^2$$

Where:

ω_{oh} is the uncoupled spanwise bending frequency.

$\omega_{o\alpha}$ is the uncoupled spanwise torsional frequency.

In the case where the surface is subjected to airflow at some supersonic Mach number, the application of Lagrange's Equations yields:

$$(24) \quad (k_h - I_h \omega^2 + i G_h + i C_h \omega) q_h - S \omega^2 q_\alpha = -\left[\int_o^\ell C_{L\alpha} q_d D_h D_\alpha C \, dy\right] q_\alpha$$

$$- S \omega^2 q_h + (k_\alpha - I_\alpha \omega^2 + i G_\alpha + i C_\alpha \omega) q_\alpha = 0$$

Using the notation:

$$(25) \quad N = \int_o^\ell C_{L\alpha} q_d D_h D_\alpha C \, dy$$

it may be observed that equations (24) lead to the determinant of Equation (10). It follows that the critical value of N needed for instability is given by Equation (14), and the frequency ω_F is given by Equation (12). A completely theoretical study of the cantilever plate may thus be performed, subject to the basic assumptions regarding the motion to be limited to that described by two degrees of freedom.

5. Ground Vibration Testing - Three-dimensional System

The relation between the ground test shaking force and the distributed aerodynamic forces which act on the plate flying at some supersonic Mach number, may be established in a manner similar to that employed in the case of the two-dimensional system. Where before the ground test input was a force, the appropriate reference input now is that of generalized force. In performing the experiment, a useful response function is the angular vibration at some reference spanwise station. Let such a vibration be found at a certain frequency to be 180 degrees out of phase with the applied force. Then allow very low density air at the chosen supersonic Mach number to flow over the surface. At the instant when the test shaker force is down, the surface is pitching nose down, and the distributed aerodynamic forces will do work on the system in the bending degree of freedom according to the expression for the generalized force.

$$N\, q_\alpha = \left[\int_0^\ell C_L\, q_d\, D_h\, D_\alpha\, c\, dy \right] q_\alpha \tag{26}$$

The net generalized force acting is then composed of the sum of the shaker and the aerodynamic inputs:

$$Q_1 = -N\, q_\alpha + P_a\, D_{ha} \,. \tag{27}$$

In order for the level of the vibration to remain at its initial test value, the test input force may now be reduced to a value P_a, such that Q_{f_2} is the same as Q_{f_1}.

The value of q_α is recognized by its effect on the reference angle $\alpha_b = D_{\alpha b}\, q_\alpha$. Then allow the density of the air to be increased far enough so that the presence of P_a is unnecessary to the maintainance of α, or q_α, and

$$Q_1 = -N\, q_\alpha \tag{28}$$

This value of Q_1 has remained the same throughout the discussion and has the value which was given it by the initial test force. Consequently:

$$P_a\, D_{ha} = -N\, q_\alpha \,. \tag{29}$$

The critical value of N, with q_α deduced from α_b, is therefore:

$$N = -\frac{P_a}{\alpha_b}\, D_{ha}\, D_{\alpha b} \tag{30}$$

It is then possible to define a critical ratio of the driving shaker force to the angle of vibration at the chosen angular pickup station.

$$(31) \qquad \frac{P_a}{\alpha_b} = \frac{C_{L\alpha}\,(.7\,p\,M_m^2)}{D_{ha}\,D_{\alpha b}} \int_0^{\ell} D_h\,D_\alpha\,c\,dy$$

Using the classical two-dimensional lift-curve slope for $C_{L\alpha}$, the critical atmospheric pressure which cannot be exceeded for any supersonic Mach number is:

$$(32) \qquad p = \frac{1}{.7\,C_{L\alpha}\,M^2} \quad \frac{D_{ha}\,D_{\alpha b}}{\int_0^{\ell} D_h\,D_\alpha\,c\,dy} \quad \frac{P_a}{\alpha_b}$$

It will be noted that the grouping of the terms shows an aerodynamic factor, a structural mode shape factor, and a dynamic response factor. The first has to be obtained directly from theory or from wind-tunnel data, while the second and third terms can be obtained from theory, from open loop ground vibration testing, or from closed loop one-channel simulator testing.

6. Flutter Simulation

The open-loop type of ground vibration test required that the angular response be monitored by the test engineer to find the frequency at which the angle was 180 degrees out of phase with the driving force. To bypass this particular part of the problem, a closed loop system may be set up which in effect causes a shaker force to be generated when the plate pitches, analagous to the aerodynamic force which is produced by an angular motion of the surface in flight. At some particular gain setting of the closed loop, an oscillation is initiated at the appropriate frequency, analogous to a flutter condition which would occur in flight if the air density and Mach number were such as to produce a certain lift per unit angular motion. The system gain in the closed loop case is given directly by the factor P_a/α_b, in pounds of driving force per unit reference angle, and the atmospheric pressure versus Mach number which defines the flutter boundary would again be found from Equation (32). The closed loop result should be the same as the open loop. But there are some differences in the process which would be significant if more

than one shaker were to be used. The components needed for the closed loop system are required to be free of phase lags over a wide frequency band. The transducer gain should be constant over a wide band. Many components suitable for getting open-loop data are inadequate for closed-loop studies. But the chief advantages of the closed-loop simulation would appear when more than one shaker would be used. As the number of shakers are increased, the system converges to a closer and closer simulation of the distributed airforces which are produced in flight.

In this report, the emphasis on the one-channel has been placed because it poses severe requirements on the components, and serves to show their successful performance under live conditions.

7. Flutter Simulation for Plate A

A study has been performed on a 30" x 12" x 1/8" cantilever plate described by the mode shape, stiffness and inertia data of Table 2. Using the data in the formula of Equation (8), the following theoretical result is obtained for the atmospheric pressure versus Mach number above which the plate would flutter.

$$p = .340 \frac{\sqrt{M^2-1}}{M^2} \tag{33}$$

An experimental result was obtained for a shaker installed at the 80% span at the mid-chord. During self-excitation, the shaker force was .265 lb., and the angle of vibration was .00128 radians. The P_a/α_a of 207 lb/radian was used in Equation (32).

$$p = \frac{\sqrt{M^2-1}}{M^2} \frac{1}{2.8} \frac{(.88)(.92)}{(140)} (207) = .427 \frac{\sqrt{M^2-1}}{M^2} \tag{34}$$

It is seen that the one-channel simulation yields a very unconservative estimate, in that the plate is supposed to be safe at an atmospheric pressure 25% greater from the simulator results as compared to a theory which incorporates inertia and stiffness data based upon the theoretical mode

shapes and measured frequencies. A number of possible explanations for this discrepancy involve the questions of:

(1) Using enough mode shapes in the theory to describe the plate as it is driven by a force at one point.

(2) The shaker force calibration.

(3) The angular pickup calibration.

It is not believed that items (2) and (3) were performed as accurately as would be needed. These techniques were poorly developed at the time. The shaker which was used in the test was modified from the original Goodman design to free the coil from a 20 lb/in. spring restraint. Such a spring was much too great relative to the spring of the primary bending mode at the shaking point, $4.13/.88^2$ or 5.31 lb/in. When the shaker was thus modified, the annulus of the magnet had to be enlarged to permit small coil mal-alignments. The force per ampere factor then became a variable which required calibration for each test. The shaker rod was preloaded against the plate and the magnitude of the preload determined by loading the rod up to breaking contact. The shaker current needed to cause chatter was then measured, to provide the force per ampere calibration factor.

The angular measuring system comprised two linear differential transformers placed at the leading and trailing edges of the plate. A transistorized phase comparator and 10 KC excitation unit served to apply the carrier to the differential transformer, and to rectify and demodulate the output signal. The output signal was fed into a transistorized power amplifier which delivered a current into the shaker in phase with the difference of the signals from the two pickups. In this investigation one of the problems which turned up and which continued to be troublesome was that of matching the gains of the two pickups. It was soon evident that matching the gains for one pair of initial positions of the pickups failed for other pairs of positions, and closer examination of the pickup calibration curves revealed slight non-linearities which accounted for the deficiencies in the system. A certain amount of carrier signal could not be filtered out of the final pickup output, and it was evident that further amplification of the output was impractical for use in a higher gain system. The phase lag in the 0-200 cps frequency band was low, but

any increase in the filtering was seen to increase the phase lag, and prevent the simulation of the no-lag lift force as a function of the angle of attack of the plate.

On the basis of the experience provided in the flutter simulation of Plate A it was concluded that a better angular pickup was needed and that it would be desirable to use an unmodified Goodman shaker for those cases in which stiff plates were to be studied.

8. Flutter Simulation for Plate B

A number of plates and root conditions were involved in some further testing, but the test assembly shown in Figure 10 was subjected to the longest series of tests for the development of suitable angular pickups, preamplifiers and power amplifiers. These units were finally all revised to meet the exacting requirements for the production of stable linear output force versus input plate angular motion.

The detection of angular displacement provided a particularly difficult problem. It was natural at first to think of two displacement pickups, as used in Plate A. When difficulties were encountered from non-linearities, the next approach was to devise a mechanical linkage which would subtract the displacements of two points on the plate spaced a certain chordwise distance apart, to produce a linear displacement proportional to the mean angle. The mean displacement was at first sensed by a linear differential transformer. For a number of reasons this arrangement was not satisfactory. Among the evils was the presence of 60 cps noise which precluded sufficient amplification for the necessary self-excitation of a stiff surface with a high supersonic flutter speed.

It was then considered that the ideal low noise - high gain pickup might be found in the phonograph realm, where such characteristics were especially prized. A crystal pickup was tried, but the phase characteristics were poor and contact of the needle on the subtraction linkage was hard to maintain. At this point a Weathers capacitance pickup was investigated. Its phase and noise characteristics were good, but it was non-linear; so it could be used only over a small distance. Precise measures of the non-linearity were not obtained, but the calibration of the pickup had to be

performed frequently, and if the gap between the face of the pickup and the moving surface changed by .010 inches, the gain changed by 10%. Different linkages were employed with this pickup. One of the more successful was a horizontal panel supported on three corner feet, Figure 6(a). Two of the feet ((1) and (2)) rested on two chordwise points on the specimen plate. The third foot (3) rested on an external fixed base, while at the fourth corner a Weathers pickup was placed directly beneath the pickup. The pickup was positioned such that when the two feet on the plate were moved equally the output voltage was zero. An output voltage would appear, then, only when the two plate feet moved differentially, i.e., when the plate took on an angular displacement. Along with this unit, a voltage preamplifier was needed, and while a D.C. device would have been desirable, it was not feasible with the shifty output from the Weathers oscillator. A low frequency A.C. preamplifier was feasible and was employed along with a D.C. transistorized power amplifier to produce a shaker current in phase with the plate angular displacement over a wide frequency band.

Another fairly successful form of an angular transducer was a vertical post mounted on the plate with a vertical plane surface. The Weathers pickup (5), Fig. (6b) placed to face the post could see it move fore and aft, but not vertically, and thus sensed angle. With the three-footed panel, questions of panel modes, faithfulness of feet contact, friction, and fixed base modes all appeared at one time or another and periodically came clanking across the scene. In the case of the vertical post-plane arrangement, the primary source of difficulty was at least reduced to the modes of that one structure, with no rubbing friction present to produce unwanted phase lags. But the fundamental non-linearity of the pickup itself was always present.

Another type of capacitance pickup was considered briefly because it was much more linear. It was recognized, however, that a mechanical structure of some kind would be necessary, and would once more provide modes to confuse the end result. For a long time, several APL engineers, namely W. Tynan and R. Hires, had been suggesting the use of optical techniques to sense the angular motion. Consideration of such techniques has been rewarding in closer attainment of a low noise, zero phase lag, high gain, modeless detection system.

The system now comprises as a light source a light beam pointer of the type used in news meeting presentations, in an arrangement shown in Figures (6c) and (10). The beam is reflected from a mirror placed vertically on the test plate, and an image is projected upon a two-photocell screen some 30 inches away. The cells are connected in parallel, with the positive and negative terminals at one end grounded, and with the signal generated at the junction of the other terminals. The signal is applied to a D.C. preamplifier, Figure 7. The signal is zero when both of the cells are illuminated equally. The output of the D.C. preamplifier is nulled for the particular pair of 6 volt batteries used as a power source. The gain control then does not change the output null. The signal is raised to .5 volts to enter the D.C. power amplifier Figure 8. This particular circuit is designed such that a steady current of .5 amperes through the shaker is provided by the input reference signal level of .5 volts from the preamplifier. A complete D.C. system is thus attained.

A complete test set-up comprised the 15.5" x 10" x .25" cantilever Plate B, clamped to a heavy aluminum block, and the one channel simulation system. The simulation system comprised the electro-optical angular pickup, the associated preamplifier, the power amplifier, and a small 3 watt, one pound force shaker. The shaker was bolted to the plate support block 12" from the root. The shaker rod was then attached to Plate B at the mid-chord. A .5 lb mass was cemented to the tip trailing edge of the plate, to provide mass unbalance. The mirror for the angular pickup was attached to the mid-chord 3/4" outboard of the shaker rod point. Token damping forces were supplied by two 1/8" screws located 3" ahead and 3" behind the mid-chord 1/2" in from the tip. The ends of the screws moved in cups of SAE 90 oil to produce damping.

The operational sequence was as follows. With the loop gain set by the preamp control, the plate was tapped lightly. The vibrations damped out; the gain was increased, and the tapping repeated. Eventually at a certain gain position, the plate continued to oscillate. At larger gains, the level of vibration was such as to exceed the 1/2 ampere limitation of the power amplifier. The peaks of the wave were clipped, and the system was in a non-linear state. At this point the oscillation had to be stopped so that the sequence of events could be repeated for the study

of the linear system. (Only cursory examination has been made so far of the tolerance in gain position for which the oscillation will be maintained in the linear regime of the feedback loop. The tolerance is apparently small.)

The next problem was to establish the gain of the loop which produced the oscillation. A direct approach was to move the photo-cell pair a known distance δ and record the change in the voltage E_p across a one ohm series resistor in the voice coil line. Using the perpendicular distance ℓ_p from the mirror to the photocell and the force per unit current λ, the force per unit angle was determined from:

$$\frac{P_a}{\alpha_b} = 2\lambda \frac{E_p}{\delta} \ell_p \tag{35}$$

Several difficulties were evident: first, the movement of the cell had to be small, so that the voltage shift would not exceed the ± .5 volt limit about the neutral .5 volt point. The movement was produced by a cell support slide pushed by the end of a micrometer, and there was some question about the fidelity of such an arrangement. The second problem arose from a shifty voltage output from the system in the high gain position. To solve these problems, the dynamic gain was established from forced vibration of the plate, as a function of gain dial reading. The modified calibration process was to determine the static reference low gain. A large movement of the photocell was necessary to produce output voltage shift of .5 volts. Further to define the input movement, a dial gage reading to increments of 1/10000 in. was placed to measure δ. The output voltage signal which fluctuated ± .02 volts about the mean value when the gain setting was high, was barely perceptible when the gain was low. Thus it was felt that the input motion and the output signal were fairly well defined for the calibration process.

In a given problem, the loop gain for plate oscillation was found by recording the gain dial reading. Then the low gain calibration was

performed to find $(E/\delta)_c$, and the preamp characteristic curve of gain ratio $\frac{(E/\delta)}{(E/\delta)_c}$ versus dial reading was used to find the gain ratio for the given test. The necessary force per unit angle was finally found from:

(36)
$$\frac{P_a}{\alpha_b} = 2\lambda \frac{\left(\frac{E}{\delta}\right)}{\left(\frac{E}{\delta}\right)_c} \left(\frac{E}{\delta}\right)_c \ell_p$$

Equation (32) was then used to define the atmospheric pressure–Mach number flutter boundary and the altitude-Mach number boundary depicted in Figure 9. Calculations for this purpose are shown in Table 5. If the lift curve slope is given by $\frac{4}{\sqrt{M^2-1}}$, then the conclusion of this study is that the plate would flutter at a Mach number of 2.9 at sea level.

9. Qualifications

At this point it would be advisable to list the qualifications on any result from the one channel simulation.

1. The flutter speed depends upon the mode shapes D_h and D_α. The shapes used in this study are simply those for a uniform cantilever. They could be improved by computations for this specific mass distribution. They could also be measured.

2. The calculation of the speed implies that flutter is taking place in a shape composed primarily of simple bending and twisting. If the second bending mode played a significant part, then the one-channel representation would fail.

3. The tip airforces for this three-dimensional system have centers of pressure ahead of the elastic axis. Again, this effect is hard to incorporate into one channel. The effect of forward centers of pressure could be assessed by moving the shaker further forward.

In special cases, to produce flutter speeds on actual missile wings, one channel might be sufficient. But to produce reasonably good results, it is the writer's opinion that at least four channels should be used on surfaces where chordwise bending is expected to be unimportant. A crude

appraisal of the significance of chordwise bending might then be achieved by the use of four more channels.

Ultimately the simulation of flutter should be helpful in checking flutter speeds by a technique which is independent of any structural vibration analysis of the given wing. Speed predictions need not be based upon legislated correlations between theoretical and experimental mode shapes and frequencies, for those cases where frequencies are close together and non-linear characteristics abound. The effects of different theoretical airforce coefficients can be appraised, and the minimum flutter speed may then be estimated.

LIST OF TABLES

TABLE 1

Two-Dimensional Flutter Analysis

$\frac{\omega_h}{\omega_\alpha}$	$\frac{\bar{x}}{c}$	$\frac{r}{c}$	μ	V_{NACA}	V_{Sim}	V_{Sim}/V_{NACA}
1.00	.10	.25	7.854	1.80	1.65	.916
1.00	.20	.25	7.854	2.20	2.34	1.065
1.00	.25	.25	7.854	2.30	2.62	1.14
.707	.10	.25	7.854	1.90	1.79	.94
.707	.20	.25	7.854	2.01	2.08	1.04
.707	.25	.25	7.854	2.20	2.26	1.03
1.00	.10	.25	7.854	2.80	2.77	.989
1.00	.20	.25	7.854	3.90	3.93	1.01
1.00	.25	.25	7.854	4.30	4.40	1.02
.707	.10	.25	7.854	3.20	3.02	.94
.707	.20	.25	7.854	3.70	3.51	.95
.707	.25	.25	7.854	3.90	3.81	.98

The Johns Hopkins University
APPLIED PHYSICS LABORATORY
Silver Spring, Maryland

TABLE 2

Basic Data for Plate A

Section	m, $\frac{\text{LB SEC}^2}{\text{IN}}$	I, LB IN.SEC^2	D_h, IN.	D_α	$m\bar{x}$, LB.SEC^2
1	.00291	.0349	.030	.153	0
2	.00291	.0349	.243	.455	0
3	.00291	.0349	.592	.740	0
4	.00291	.0349	1.000	1.000	0
Tip	.00162	.206	1.200	1.140	.0174

I_h = .00641 LB. IN. SEC^2 k_h = 4.13 LB IN. ω_h^2 = 645 RAD^2/SEC^2

I_α = .330 LB IN. SEC^2 k_α = 1315 LB. IN. ω_α^2 = 3990 RAD^2/SEC^2

TABLE 3

Mode Shape Data for Plate B

	D_h	D_α	$D_h D_\alpha$
0	0	0	0
.100	.0336	.1737	.00583
.200	.1277	.3256	.04158
.300	.2730	.4965	.1282
.400	.4598	.6018	.2767
.500	.6791	.7071	.4802
.600	.9223	.8090	.7461
.700	1.1818	.8910	1.0529
.800	1.4510	.9511	1.3800
.900	1.7248	.9877	1.7036
1.000	2.0000	1.0000	2.0000

$$\int_0^{\ell} D_h^2 \, dy = 1.00\,\ell$$

$$\int_0^{\ell} D_\alpha^2 \, dy = .50\,\ell$$

$$\int_0^{\ell} D_h D_\alpha \, dy = .6214\,\ell$$

TABLE 4

Plate B

Theoretical Inertia and Stiffness Data

INERTIA

Location	$\bar{y}$, IN	$\bar{x}$, IN	η	Δw, LB.	D_h, IN.	D_α	D_h^2	D_α^2	$D_h D_\alpha$
a	12	0	.775	.00221	1.3837		1.9146		
b	12.75	0	.825	.100	1.519	.9603	2.3074		
d	14.875	4.375	.960	.500	1.8899	.9951	3.5717	.9902	1.8806

$$I_h = I_{oh} + \frac{\Sigma \Delta w D_h^2}{386}$$

$$I_h = .0100 + \frac{2.0208}{386}$$

$$I_h = .0152 \text{ LB. IN SEC.}^2$$

$$I_\alpha = I_{o\alpha} + \frac{\Sigma \Delta w \bar{x} D_\alpha}{386}$$

$$I_\alpha = .0417 + \frac{.50 (4.38)^2 (.990)}{386}$$

$$I_\alpha = .0663 \text{ LB. IN. SEC.}^2$$

$$S = \frac{\Delta w \bar{x} D_h D_\alpha}{386}$$

$$S = \frac{.50 (4.38) (1.881)}{386}$$

$$S = .0107 \text{ LB IN.}$$

STIFFNESS

k_h = 477 LB. IN.

k_α = 18400 LB. IN.

These have been determined such that the coupled frequencies agree with the measured values of 28 and 89.5 cps for the "bending" and "torsion" modes respectively.

TABLE 5

Flutter Boundary Data, Plate B

Atmospheric Pressure Vs. Mach No.

Altitude Vs. Mach No.

Reference Figure 9

Ref. Equation 32

$$p = \frac{1}{.7\, C_{L\alpha}\, M^2} \frac{D_{ha}\, D_{\alpha b}}{\int_0^{\ell} D_h\, D_\alpha\, c\, dy} \left(\frac{P_a}{\alpha_b}\right)$$

$$p = 44.9 \frac{\sqrt{M^2-1}}{M^2} \qquad M > 1.5$$

Ref. Table 3

$D_{ha} = 1.38$

$D_{\alpha b} = .960$

$$\int_0^{\ell} D_h\, D_\alpha\, c\, dy = 15.5\ (10)\ (.6214)$$

$$C_{L\alpha} = \frac{4}{\sqrt{M^2-1}}$$

Ref. Equation 36

$$\frac{P_a}{\alpha_b} = 2\lambda \left[\frac{\left(\frac{E}{\delta}\right)}{\left(\frac{E}{\delta}\right)_c}\right] \left(\frac{E}{\delta}\right)_c \ell_p$$

λ = .85 lb/amp for this shaker.

$$\frac{\left(\frac{E}{\delta}\right)}{\left(\frac{E}{\delta}\right)_c} = \frac{.156}{.018}$$

$$\left(\frac{E}{\delta}\right)_c = 21.3$$

$$\ell_p = 29$$

P_a/α_b = 9100 lb/radian.

LIST OF FIGURES

FIGURE 1

Airforces on

A Two Dimensional System

Airforce = $N_{\alpha} + C_{a}\dot{h}$

Moment = $C_{\dot{\alpha}}$

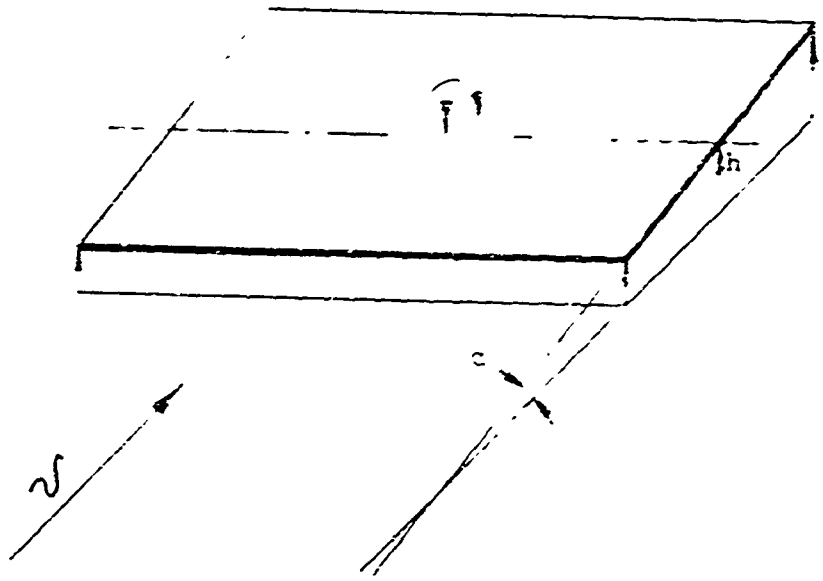

FIGURE 2

Shaker Force - Airforce Relation

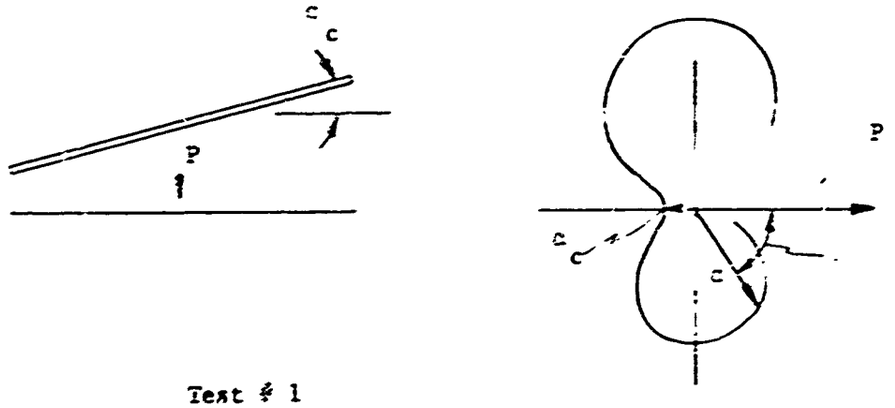

Test # 1

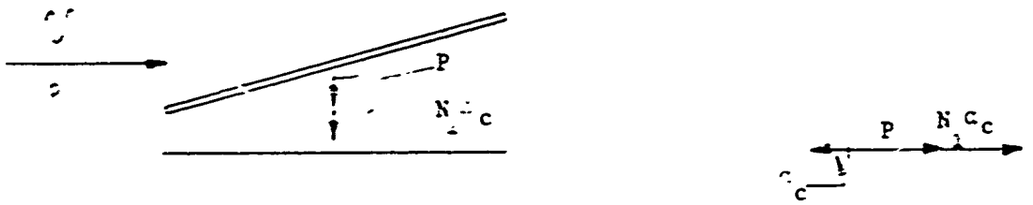

Test # 2

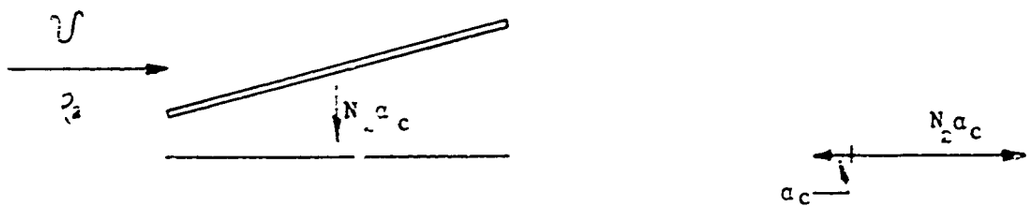

Test # 3

FIGURE 3

Airforces vs. Simulator Forces

Plate B

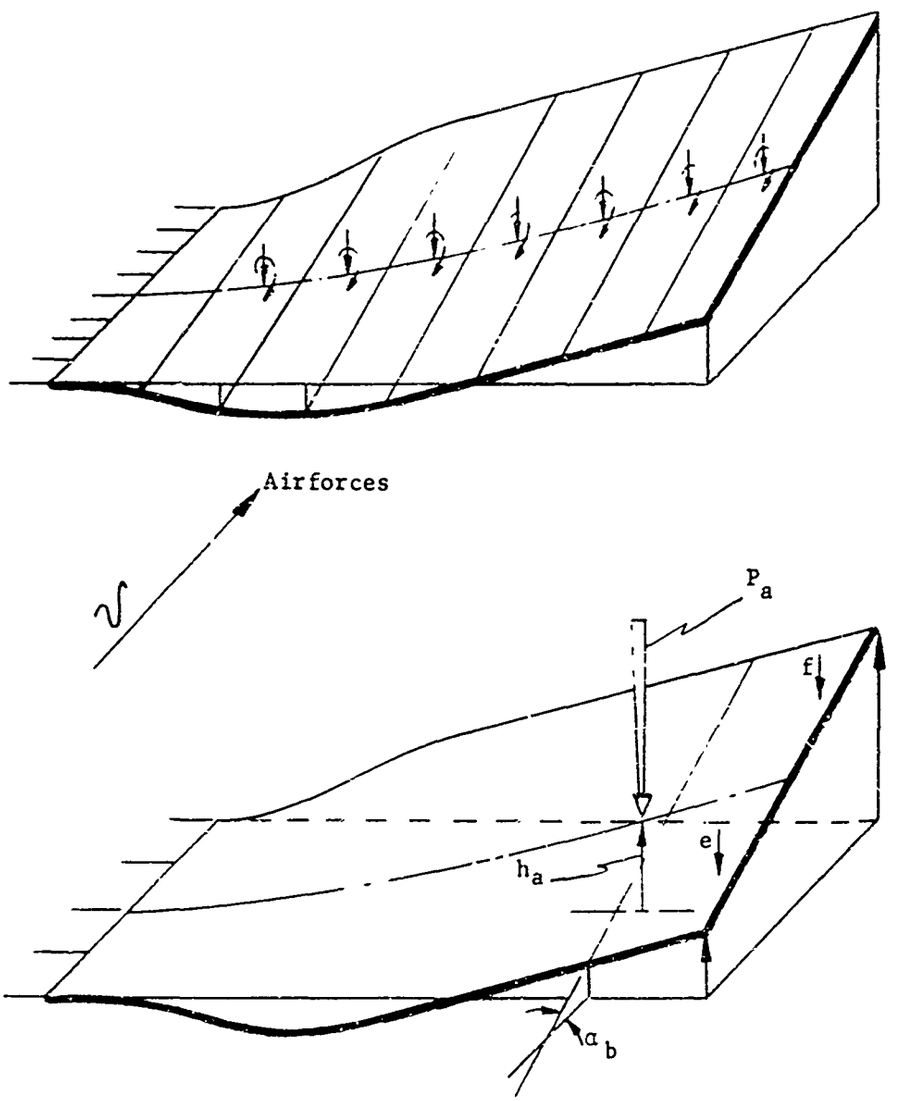

Simulator Forces

FIGURE 4

Planform - Plate B

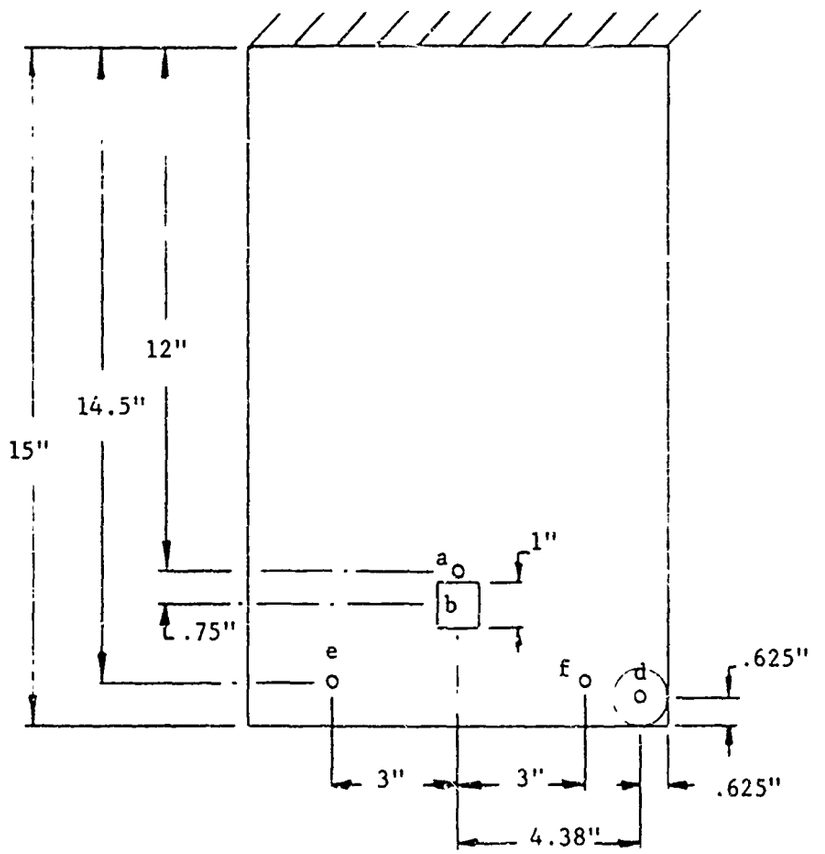

FIGURE 5

Flutter Simulator

Block Diagram - One Channel

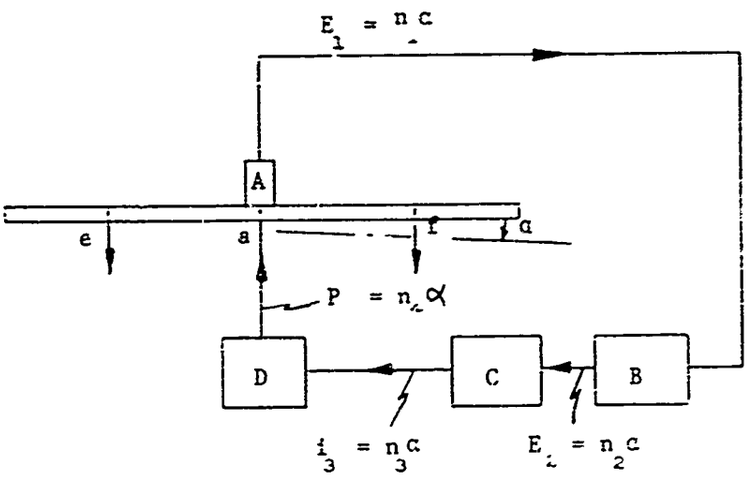

A - Angular Vibration Transducer

B - Preamplifier

C - Power Amplifier

D - Shaker

e - Forward Damper

f - Rear Damper

FIGURE 6

Three Angular Pickups

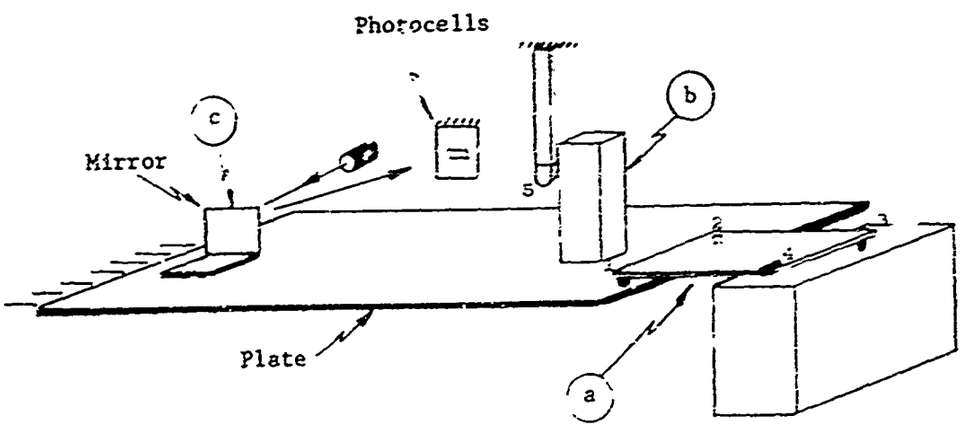

4 Capacitance Pickup
5 " "

FIGURE 7

Preamplifier

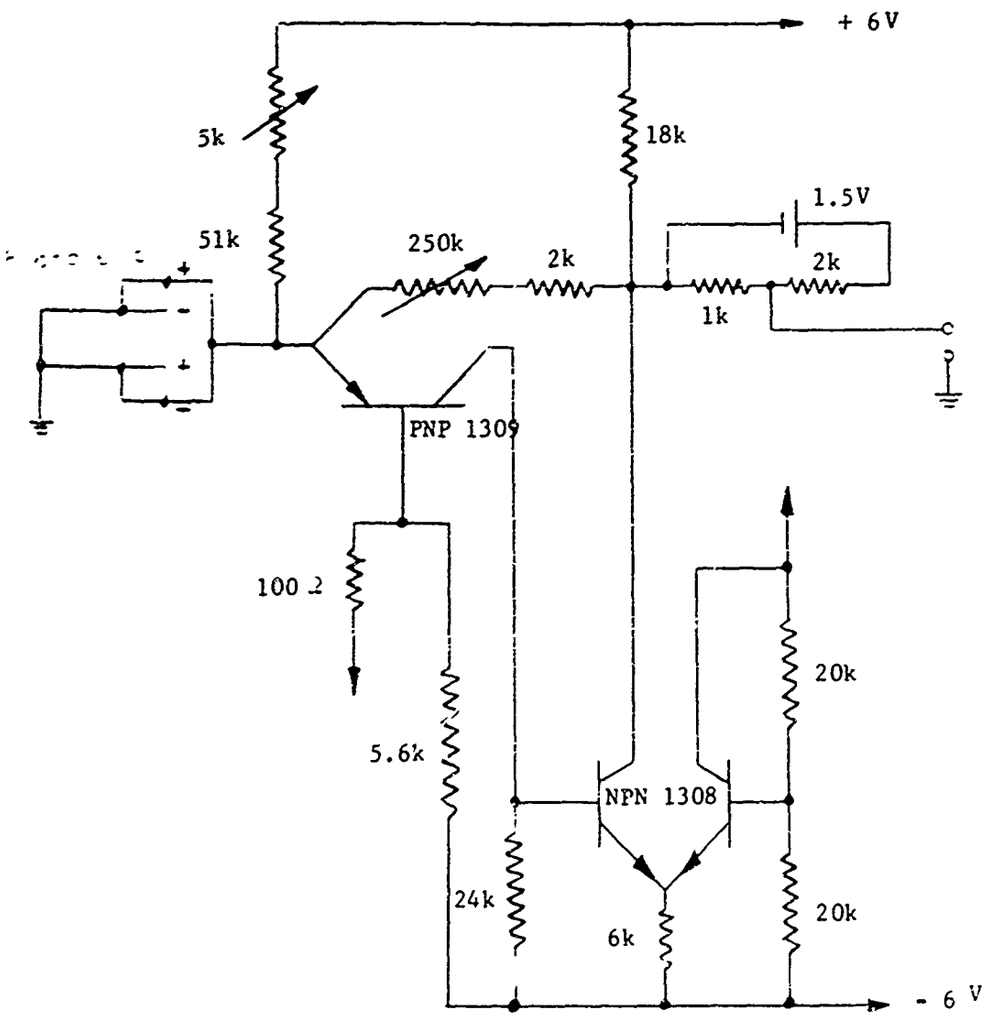

FIGURE 8

Bush Power Amplifier

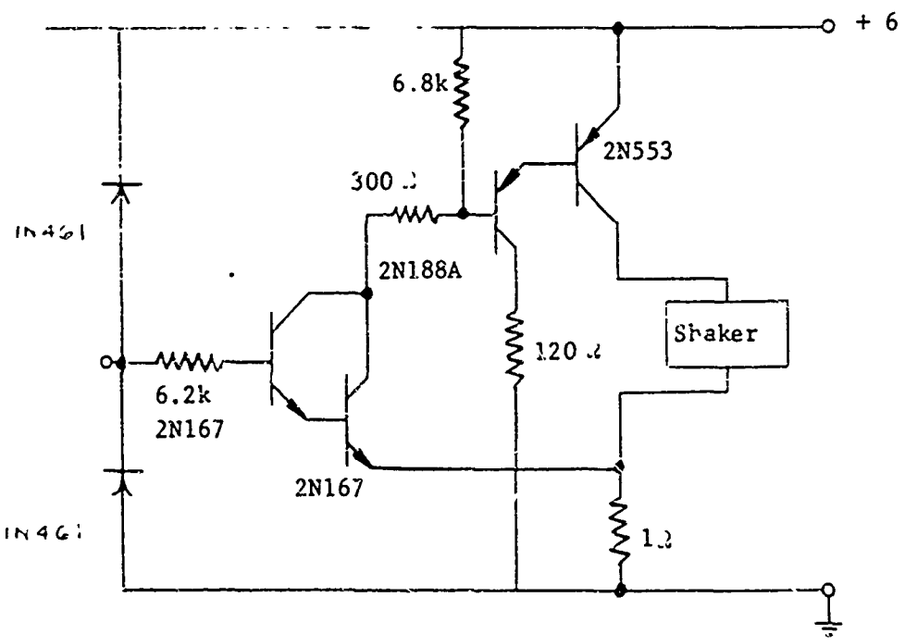

FIGURE 9

Plate B Flutter Boundary

Atmospheric Pressure vs. Mach No.

and Altitude vs. Mach No.

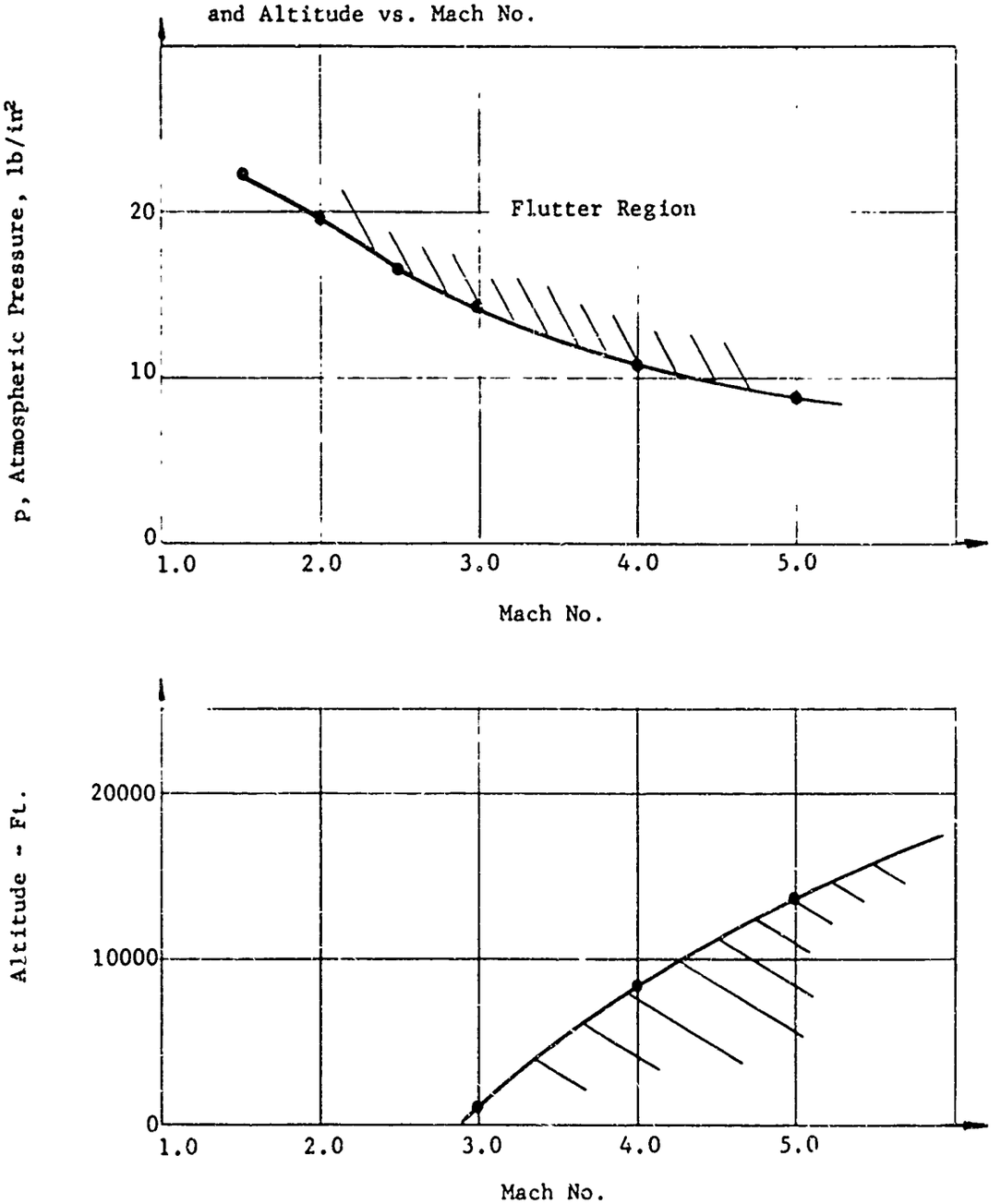

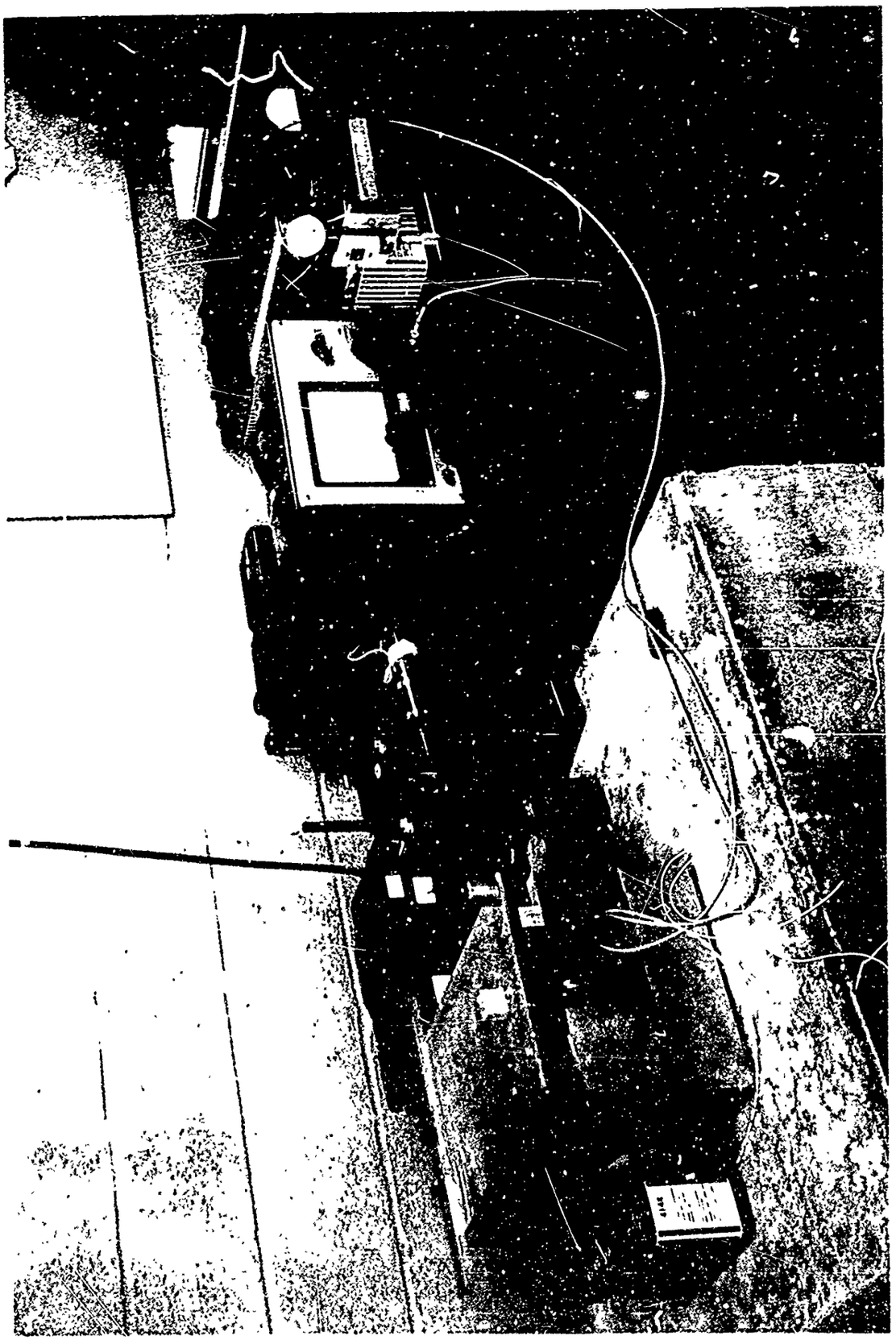

FIGURE 10

PLATE B FLUTTER SIMULATION TEST

REFERENCES

(1) NACA Report No. 846, 1946,
"Flutter and Oscillating Airforce Calculations for an Airfoil in a Two-Dimensional Supersonic Flow" by I. E. Garrick and S. I. Rubinow.

(2) "Piston Theory - A New Aerodynamic Tool for the Aeroelastician" by Holt Ashley and Garabed Zartarian, Journal of the Aeronautical Sciences, December 1956.

ACKNOWLEDGEMENT

The development of the flutter simulator has been supported by Bureau of Naval Weapons, RMGA.

The electronic design, which is the heart of the system, has been done in its entirety by Mr. George Bush of APL.

The suggestions for the use of electro-optical angular measurement were made by Mr. W. A. Tynan, Mr. R. G. Hires, both of APL, and by Mr. C. M. Kearns, Jr. of the United Aircraft Corporation.

Mr. James Kilchenstein, APL, has contributed many helpful suggestions and loyal assistance in this enterprise.